buildings

MDPI

Article

Impacts of Hydrogen Blending on High-Rise Building Gas Distribution Systems: Case Studies in Weifang, China

Yitong Xie [1,2], Xiaomei Huang [1,3,4,5,*], Haidong Xu [6], Guohong Zhang [7], Binji Wang [1], Yilin Zhao [1] and Fengwen Pan [8]

[1] School of Civil Engineering, Chongqing University, Chongqing 400045, China; xieyitong1996@icloud.com (Y.X.); 202316131408@stu.cqu.edu.cn (B.W.); sc990309@126.com (Y.Z.)
[2] Chongqing University Industrial Technology Research Institute, Chongqing 400045, China
[3] Joint International Research Laboratory of Green Buildings and Built Environments (Ministry of Education), Chongqing University, Chongqing 400045, China
[4] National Centre for International Research of Low-Carbon and Green Buildings (Ministry of Science and Technology), Chongqing University, Chongqing 400045, China
[5] State Key Laboratory of Safety and Resilience of Civil Engineering in Mountain Area, Chongqing 400045, China
[6] Weifang Municipal Public Utility Service Center, Weifang 261000, China; dong56693@163.com
[7] Weifang Gaoxin China Resources Gas Co., Ltd., Weifang 261000, China; zghzbcrg@163.com
[8] National Center of Technology Innovation for Fuel Cell, Weifang 261000, China; panfengwen@outlook.com
* Correspondence: hxm1980@cqu.edu.cn

Abstract

Hydrogen is widely regarded as a promising clean energy carrier, and blending hydrogen into existing natural gas pipelines is considered a cost-effective and practical pathway for large-scale deployment. Supplying hydrogen-enriched natural gas to buildings requires careful consideration of the safe operation of pipelines and appliances without introducing new risks. In this study, on-site demonstrations and experimental tests were conducted in two high-rise buildings in Weifang to evaluate the impact of hydrogen addition on high-rise building natural gas distribution systems. The results indicate that hydrogen blending up to 20% by volume does not cause stratification in building risers and leads only to a relatively minor increase in additional pressure, approximately 0.56 Pa/m for every 10% increase in hydrogen addition. While hydrogen addition may increase leakage primarily in aging indoor gas systems, gas meter leakage rates under a 10% hydrogen blend remain below 3 mL/h, satisfying safety requirements. In addition, in-service domestic gas alarms remain effective under hydrogen ratios of 0–20%, with average response times of approximately 19–20 s. These findings help clarify the safety performance of hydrogen-blended natural gas in high-rise building distribution systems and provide practical adjustment measures to support future hydrogen injection projects.

Keywords: hydrogen-enriched natural gas; distribution system; high-rise building; clean energy

Check for updates

Academic Editor: Apple L.S. Chan

Received: 5 December 2025
Revised: 7 January 2026
Accepted: 8 January 2026
Published: 10 January 2026

Copyright: © 2026 by the authors. Licensee MDPI, Basel, Switzerland. This article is an open access article distributed under the terms and conditions of the Creative Commons Attribution (CC BY) license.

1. Introduction

In recent decades, the rapid increase in carbon dioxide (CO_2) and methane (CH_4) emissions has posed significant challenges to climate change mitigation and global sustainability. To address these challenges, it has become increasingly important to reduce dependence on fossil fuels and accelerate the deployment of low-carbon energy systems [1]. Owing to its carbon-neutral nature and high versatility as both an energy carrier and storage medium [2],

hydrogen has emerged as a promising clean energy solution [3]. Many countries have incorporated hydrogen into national energy strategies and conducted extensive research and industrial demonstration projects. It is predicted that hydrogen could contribute to around 20% of global CO_2 emission reduction by 2040 [4] and more than 15% of total energy demand by 2050 [5].

The hydrogen value chain typically consists of three stages: production [6], transportation [7], and end-use application [8]. At present, hydrogen is predominantly produced from fossil fuels and industrial by-product gases, while renewable hydrogen is regarded as the ultimate development goal [9]. Hydrogen can be transported via high-pressure tankers, hydrogen pipelines, or by blending into existing natural gas networks. Considering the limited transport capacity and short delivery range of high-pressure tankers [10], as well as the high capital cost and long construction period associated with hydrogen pipelines [11], injecting hydrogen into natural gas pipelines for end-user consumption is a cost-effective and practical approach [12]. This strategy can enhance the resilience and operational flexibility of both the gas and electricity systems [13,14], while reducing infrastructure expansion and capital investment.

Hydrogen and natural gas exhibit significant differences in physical and chemical properties, including density, diffusion coefficient, and flammability limits. The allowable hydrogen blending ratio in natural gas pipelines has not yet been fully established. Supplying hydrogen-enriched natural gas to buildings requires ensuring the safe operation of pipelines and appliances without introducing new risks. In building gas distribution systems, lower gas density after hydrogen blending increases the additional pressure in risers, which may potentially adversely affect combustion stability in end-use appliances. The density difference will also cause stratification in tall risers, leading to non-uniform gas composition and unstable flames. In addition, the high diffusivity of hydrogen may increase leakage in indoor gas systems and degrade airtightness. Changes in gas properties can also influence the performance of gas alarms, potentially reducing detection accuracy and increasing safety risks. These challenges are expected to become more pronounced in high-rise buildings due to greater riser height. Therefore, systematic investigation of distribution system performance under hydrogen-enriched natural gas conditions is required.

Several countries, including the Netherlands [15], Spanish [16], Italy [17], Canada [18,19] and Australia [20–22] have carried out pilot projects to evaluate the suitability of existing pipelines and appliances for hydrogen blending. The results indicate that the airtightness, durability and operational safety of the transmission system are not significantly affected, and gas appliances could operate normally with the hydrogen ratio up to 20%. However, these projects were primarily implemented in low-density residential areas with low-rise houses, resulting in a notable lack of research evidence for high-rise building applications.

Previous studies have reported that gas mixtures may undergo gravitational stratification under certain conditions. However, such effects become significant only under extremely high gravitational fields (greater than 10^{11} g) or height differences exceeding 100 km, and require decades to reach equilibrium [23]. Therefore, short-term standing does not lead to noticeable stratification [24], and the effect can generally be neglected in engineering practice [25,26]. By contrast, other studies suggest that, in enclosed spaces, hydrogen-enriched natural gas may exhibit a tendency toward stratification [27–29], with the stratification extent increasing with hydrogen ratio and pressure, and decreasing with riser diameter, height, and temperature [30]. At present, the stratification behavior of hydrogen-enriched natural gas remains uncertain, as the reliability of theoretical models has not been fully validated and numerical simulations struggle to reproduce the dynamic balance between gravity and intermolecular interactions. Therefore, on-site experiments are required to evaluate whether stratification occurs under real building operating conditions.

Leakage can occur in natural gas systems even when overall pipeline integrity remains relatively good, and the leakage rate of polyethylene (PE) pipes is generally higher than that of steel pipes [31]. Some studies have shown that under low-pressure conditions, the leakage rates of hydrogen-enriched natural gas and natural gas are similar [32], which can be explained by the dynamic equilibrium at the leakage path inlet and the non-equilibrium transport mechanisms within the leakage path [33]. Other studies observed an increase in leakage rate with rising hydrogen ratio, although the increase was relatively small and did not pose significant safety concerns [34]. Leakage is found mainly at fittings such as valves, and low hydrogen ratios do not substantially increase the leakage rate at these locations. However, particular attention should be paid to elastomer sealing materials, as materials such as natural rubber and styrene–butadiene rubber exhibit poorer sealing performance against hydrogen [35]. It should be noted that most existing studies were conducted on new pipelines and components. In real distribution networks, pipelines, fittings, and sealing materials may have been in service for decades, during which aging and mechanical degradation can significantly reduce airtightness. Therefore, experimental evaluation of the airtightness of in-service pipelines and fittings is required to accurately assess the impact of hydrogen blending in practical applications.

From the foregoing analysis, it is evident that most existing research has focused on evaluating the effects of hydrogen blending on transmission systems through pilot demonstrations, as well as experiments and simulations conducted on new pipelines and fittings. However, studies specifically targeting gas distribution systems in high-rise buildings remain limited. Owing to the much lower density and higher diffusion coefficient of hydrogen compared with methane, hydrogen addition may alter gas distribution behavior in tall pipelines, potentially leading to stratification. In addition, the associated reduction in gas density can increase buoyancy-induced pressure in high-rise systems, while the wider flammability range of hydrogen raises additional concerns regarding leakage-related safety risks. In this study, on-site experiments were carried out in two residential high-rise buildings in Weifang to evaluate the impact of hydrogen addition on high-rise building natural gas distribution systems. The distribution systems were modified to enable real-time hydrogen blending. Experiments and theoretical analyses were conducted on riser stratification, additional pressure, indoor system airtightness, and the effectiveness of domestic gas alarms. The findings clarify the safety implications of hydrogen blending in high-rise building gas distribution systems and provide corresponding adjustment measures to support future hydrogen injection projects.

2. Methodology

2.1. Gas Properties

The natural gas composition in this study is shown in Table 1. A comparison of the properties of hydrogen and methane is appropriate for analysing the effects of hydrogen addition to natural gas, as methane is the primary component of natural gas, as shown in Table 2. The density, heating value and Wobbe index are measured under room condition (298 K, 1 atm).

Table 1. Natural gas composition.

Composition	Methane	Ethane	Propane	n-Butane	Iso-Butane	n-Pentane	Iso-Pentane	Neo-Pentane
Formula	CH_4	C_2H_6	C_3H_8	n-C_4H_{10}	i-C_4H_{10}	n-C_5H_{12}	i-C_5H_{12}	NeoC_5H_{12}
Volume percentage (%)	94.3152	3.6051	1.3192	0.2864	0.3487	0.0238	0.0089	0.0025

Table 2. Gas properties of methane and hydrogen.

	Methane	Hydrogen	Methane/Hydrogen Ratio
Density (kg/m^3) [36]	0.648	0.0813	7.97
Volumetric stoichiometric air requirement (m^3/m^3)	9.52	2.38	4.00
Low heating value (MJ/m^3) [37]	34.0	10.2	3.33
High heating value (MJ/m^3) [37]	37.8	12.5	3.02
Low flammability (%) [38]	5	4	1.25
High flammability (%) [38]	15	75	0.20
Wobbe index (MJ/m^3) [39]	51.9	48.5	1.07
Diffusion coefficient [40]	0.20	0.63	0.32

The heating value of hydrogen is significantly less than that of methane; however, its lower density leads to a higher volumetric flow rate under the same pressure conditions, as described by Bernoulli's principle. Combining these two effects, the Wobbe index is introduced to quantify the change in heat load when the gas supply pressure is consistent, which is defined as the division of heating value and the square root of relative density [41]. The Wobbe indexes of hydrogen and methane are similar, which indicates that limited burner heat load variation with constant gas supply pressure is acceptable.

The density of hydrogen is much lower than that of methane, and its diffusion coefficient is significantly higher, which may cause gas stratification in taller pipelines. The resulting higher hydrogen concentration could exceed the limit, leading to unstable combustion of gas appliances [36]. In addition, the reduction in gas density with increasing hydrogen ratio leads to higher additional pressure, potentially causing the gas pressure for high-rise users to exceed the design value. Moreover, due to the much wider flammability range of hydrogen, greater attention should be given to leakage prevention measures to avoid potential hazardous incidents.

2.2. Case Description

In this study, two residential buildings in Weifang were selected for field experiments. Weifang, a northern city in China, boasts a strong industrial foundation and high gas penetration, with pipeline natural gas being the primary supply in the urban area. The local climate is moderate, with no frequent extreme weather conditions. The city's gas pipeline network and building distribution system can reasonably represent typical urban natural gas distribution systems across most regions of China.

The first building has 16 floors with a floor height of 3 m, comprising 128 households, and is currently unoccupied. The second building has 11 floors with the same floor height, accommodating 44 households, and is currently inhabited. Each building is equipped with an individual pressure regulator installed outside. With heights exceeding 30 m, these two buildings provide a suitable setting for investigating the impacts of hydrogen blending on high-rise building gas distribution systems. In addition, the two buildings represent different operating conditions of indoor gas systems, with one building unoccupied and the other under normal residential use. This allows a preliminary comparison between relatively inactive systems and in-service systems with daily gas consumption. Although the sample size is limited, the selected buildings are considered representative of typical high-rise residential gas distribution systems in northern Chinese cities.

2.3. Gas Supply

A large volume of gas was required for the building tests, so a mobile hydrogen injection appliance was employed. After minor modifications to the building distribution system, hydrogen-enriched natural gas was supplied to the entire building. The gas supply system is illustrated in Figure 1. In the original configuration, urban medium-pressure natural gas (~0.35 MPa) flowed through the regulator, which was equipped with upstream

and downstream valves, reducing the pressure to 3 kPa before entering the building's gas riser. After modification, a hydrogen injection system was installed, consisting of the hydrogen injection appliance and two valves positioned upstream and downstream.

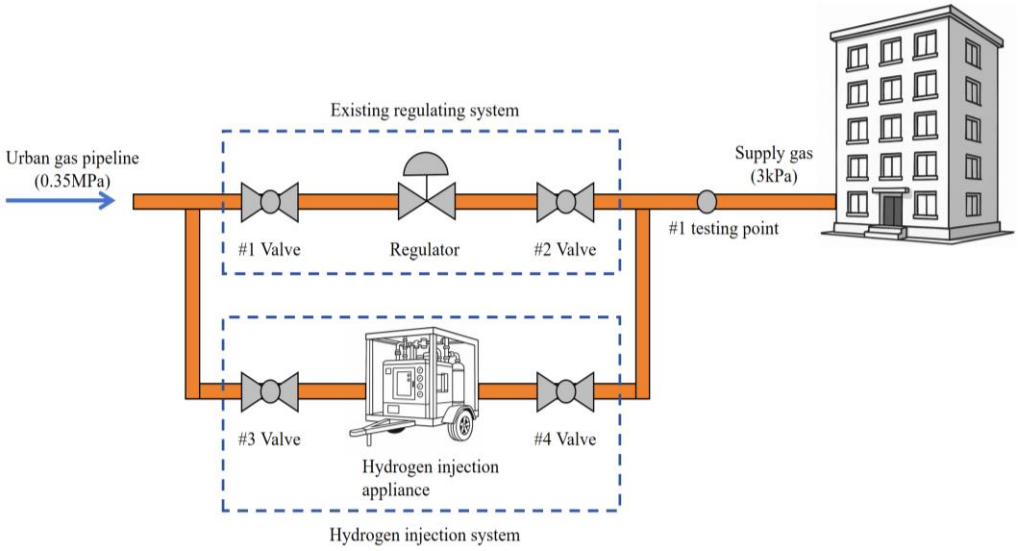


Figure 1. Schematic illustration of the building gas supply system.

The hydrogen injection appliance is shown in Figure 2a, with the hydrogen cylinders mounted on it. The main performance parameters are listed in Table 3. Initially, the outlet pressure of the hydrogen cylinder is adjusted to closely match the natural gas pressure in the pipeline (within 0.05 MPa). Then the pressures of hydrogen and natural gas are balanced by a balancing valve. Subsequently, hydrogen and natural gas are mixed at a preset ratio controlled by a proportioning valve, and the mixture enters a buffer tank under the control of an electromagnetic valve. When the buffer tank pressure exceeds the upper limit, the mixing process automatically stops. As gas is consumed and the pressure falls below the lower limit, the appliance restarts mixing. This cyclic process ensures a stable and uniform hydrogen–natural gas mixture under varying flow conditions.



(**a**) (**b**)

Figure 2. On-site gas supply system: (**a**) Hydrogen injection appliance; (**b**) Pipeline modification.

During the gas system modification, a branch was added to the tee joint upstream of Valve #1 to connect the inlet of the hydrogen injection appliance, and a new tee joint was installed on the low-pressure supply pipe near the riser to connect its outlet. Valves were installed both upstream and downstream of the hydrogen injection appliance. The on-site gas system after modification is shown in Figure 2b. When the building was supplied with natural gas, Valves #1 and #2 remained open, while Valves #3 and #4 were closed, and the hydrogen injection appliance was inactive. During the experiments, Valve #3 was opened

to provide natural gas to the hydrogen injection appliance, and hydrogen was supplied from the cylinders mounted on it. Once the hydrogen–natural gas mixture reached the preset ratio, Valve #4 was gradually opened. After a period of stable operation, Valves #1 and #2 were gradually closed, supplying the building with hydrogen-enriched natural gas. At the end of the experiments, Valves #1 and #2 were reopened, while Valve #3 and the hydrogen cylinder were closed. Once the mixture in the buffer tank was released, Valve #4 was closed, restoring natural gas supply to the building.

Table 3. Performance parameters of the hydrogen injection appliance.

No.	Metrics	Parameter
1	Dimensions	2.6 × 1.5 × 2 m (L × W × H)
2	Hydrogen percentage	0–30%
3	Accuracy	±0.5%
4	Operating pressure	0.08–0.18 MPa
5	Inlet pressure	0.2–1.0 MPa
6	Outlet pressure	0.2–0.3 MPa, 1–5 kPa
7	Relief pressure	1.33 MPa
8	Output flow rate	0–30 Nm^3/h

2.4. Test Procedure

The main experiments conducted in this study include the stratification in the gas riser, the additional pressure in the gas distribution system, the airtightness of indoor pipelines and appliances, and the effectiveness of in-service domestic gas alarms. The corresponding test procedures are described below.

1. Stratification in the gas riser

Previous studies have primarily investigated stratification in enclosed test chambers or large-volume spaces. In this study, stratification experiments were conducted directly in a vertical building gas riser, which better represents high-rise pipelines with large height-to-diameter ratios. The stratification experiment of the gas riser was conducted in Building #1 under a 20% hydrogen blending ratio. The test method is illustrated in Figure 3. The building gas riser was made of galvanized steel pipe, and a diameter reduction was applied at the midpoint of the riser to mitigate the effect of additional pressure, changing from DN40 (Floors 1–8) to DN25 (Floors 9–16). To represent the maximum possible concentration difference along the riser, gas composition measurements were conducted at the 3rd and 16th floors, corresponding to the lower and upper extremes of the vertical pipe, where gravitational stratification effects are theoretically most pronounced. The stratification tests were performed under static conditions after gas supply stabilization in order to primarily isolate gravity-driven effects and the influence of user gas consumption and flow-induced mixing was not considered in this experiment.

Once the gas distribution system was supplied with hydrogen-enriched natural gas, the stratification test was conducted according to the following procedure:

(1) Methane and hydrogen concentrations were initially measured at testing points #2 and #4 using the gas composition analyzer;
(2) Valve #5 was then closed to isolate the riser and initiate the standing condition;
(3) After a standing period exceeding 12 h, methane and hydrogen concentrations at the same testing points were measured again to evaluate potential stratification effects.

The gas composition analyzer used in the experiment was a Gasboard-3100P, which applies infrared absorption spectroscopy to achieve simultaneous detection of multiple gas components with high sensitivity and accuracy.

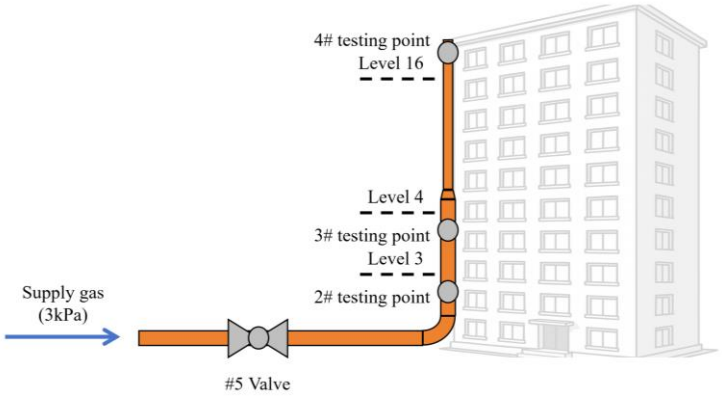


Figure 3. Schematic illustration of the riser stratification test.

2. Additional pressure in the gas distribution system

To investigate the effect of hydrogen addition on the additional pressure in high-rise building gas distribution systems, experiments were conducted in Building #1 under hydrogen blending ratios of 0% and 20%. After the gas supply was stabilized, static pressure measurements were carried out following the steps below:

(1) The pressure at the 4th floor (#3 testing point in Figure 3) was measured using a micro-manometer;
(2) The pressure at the 16th floor (#4 testing point in Figure 3) was subsequently measured under the same operating conditions;
(3) The additional pressure per unit height was then calculated based on the measured pressure difference and the corresponding floor height:

$$\Delta P_t = \frac{P_t - P_b}{n \times h_f} \quad (1)$$

where ΔP_t is additional pressure per unit height, Pa/m; P_t is the pressure at the top of the riser, Pa; P_b is the pressure at the bottom of the riser, Pa; n is the number of floors; h_f is the floor height, m.

The micro-manometer used in the experiments was a Testo-510 (Testo SE & Co. KGaA, Titisee-Neustadt, Germany), which enables high-precision measurement of small pressure differences. In addition, the instrument features temperature and air density compensation functions, ensuring reliable measurement accuracy, and is widely used in industrial applications.

3. Airtightness of indoor pipelines and appliances

To evaluate the effect of hydrogen addition on the airtightness of indoor gas systems, experiments were conducted in Building #1 under hydrogen ratios of 0%, 10%, and 20%. The airtightness tests were performed on the indoor gas system downstream of the gas meter, including pipelines, appliance connections, and associated fittings, using the pressure decay (static pressure drop) method. In this study, the measured leakage rate represents the integrated leakage behavior of the in-service indoor gas system rather than isolated leakage from individual components, with the objective of assessing the overall airtightness performance under hydrogen-enriched natural gas conditions. The test procedure consisted of the following steps:

(1) A high-precision pressure sensor and a temperature sensor were installed on the downstream pipeline, as shown in Figure 4;
(2) The gas valve was opened and the gas cooktop was briefly operated to ensure the system was fully filled with hydrogen-enriched natural gas;

(3) The downstream valve of the gas meter was then closed to isolate the test section;
(4) Gas pressure and temperature were continuously recorded for a period of 30 min.

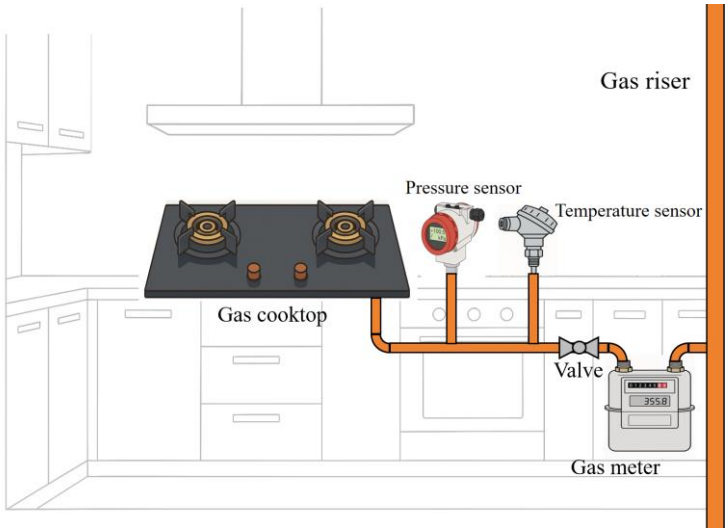


Figure 4. Schematic illustration of the airtightness test rig.

The pressure sensor used in the experiments was an industrial-grade pressure transmitter (SUP-P3000, Supmea Automation Co., Ltd., Hangzhou, China), which employs a piezoresistive sensing element combined with a stainless-steel isolation diaphragm to ensure high stability and long-term reliability. The temperature sensor was a resistance temperature detector (SUP-TSR, Supmea Automation Co., Ltd., Hangzhou, China), characterized by excellent durability and measurement stability, making it suitable for long-term applications.

The gas temperature is above 0 °C and the pressure is below 4 bar, which can reasonably be regarded as an ideal gas. According to the ideal gas law, the total leakage from indoor pipeline, appliances and fittings can be calculated by the measured real-time pressure and temperature:

$$\Delta m = \frac{M(P_1 - P_2)V}{RT} \tag{2}$$

where Δm is the total gas leakage mass, kg; M is the molecular weight of the gas, g/mol; P is the gas pressure, Pa; V is the pipeline volume, m^3; R is ideal gas constant, 8.314 J/mol·K; T is the gas temperature, K; Subscripts 1 and 2 denote the conditions before and after the test, respectively.

The volumetric leakage rate at standard conditions can be calculated as:

$$Q = \frac{T_0}{T}\frac{(P_1 - P_2)V}{\tau P_0} \tag{3}$$

where Q is the volumetric leakage rate at standard conditions, m^3/s; T_0 is the standard temperature, 293.15 K; P_0 is the standard pressure, 101,325 Pa; τ is the time interval between the initial and final measurements, s.

During the pilot project conducted on Building #2 under a 10% hydrogen ratio, a subset of residents was selected for gas meter airtightness testing to evaluate the effect of hydrogen addition. A sealed plastic bag was placed over each gas meter to form an enclosed space, isolating the gas inside the bag from the external environment. If leakage occurred, the leaked gas would gradually accumulate inside the bag. The concentrations of methane and hydrogen in the bag were then measured, from which the gas meter leakage rate was calculated.

4. Effectiveness of domestic gas alarms

The experiments were conducted on Building #1 under hydrogen ratios of 0%, 10% and 20% to investigate the effect of hydrogen addition on the effectiveness of in-service domestic gas alarms. The tested alarms were conventional catalytic combustion-based methane detectors, which are widely used in residential buildings in China. The leakage source with a diameter of 1 mm was positioned 1 m below the gas alarm to simulate the leakage scenario and the alarm response time was recorded.

3. Results and Discussion

3.1. Stratification in the Gas Riser

The density of hydrogen is much lower than that of natural gas, so hydrogen tends to diffuse upward under the influence of gravity, which can potentially lead to gas stratification in hydrogen-enriched natural gas. Stratification is more likely to occur during periods of low gas demand, when the gas remains static in the pipeline. Such compositional differences can lead to a hydrogen ratio exceeding the preset limit, resulting in potential safety risks. The stratification can be analyzed using the Boltzmann distribution theory [23]. In a rigid vertical pipe filled with ideal gases, the normalized probability density of a gas is given by:

$$\rho_{\mathrm{i}}(h) = \frac{e^{-\frac{M_i g h}{RT}}}{\int_0^H e^{-\frac{M_i g h}{RT}} dh} \tag{4}$$

where $\rho_{\mathrm{i}}(h)$ is the normalized probability density of gas i at height h; m_{i} is the mass of the gas molecular, kg/mol; g is gravitational acceleration, m/s^2; h is the height of gas, m; H is the maximum height of the pipe, m.

Assuming ideal gas equation of state, the distribution of partial pressure of gas can be calculated as:

$$P_i(h) = P^{tot} F_i^{tot} \rho_i(h) H \tag{5}$$

where $P_{\mathrm{i}}(h)$ is the partial pressure of gas i at height h, Pa; P^{tot} is the average pressure of the whole system, Pa; ${F_i}^{\mathrm{tot}}$ is the volume fraction of gas i in the whole system.

Then the distribution of volume fraction can be calculated as:

$$F_i(h) = \frac{F_i^{tot} \rho_i(h)}{\sum F_i^{tot} \rho_i(h)} \tag{6}$$

where $F_{\mathrm{i}}(h)$ is the distribution of volume fraction of gas i at height h.

The effect of hydrogen ratio and pipeline height on gas stratification is calculated, as shown in Figure 5. The hydrogen fraction deviation was plotted on the y-axis to represent the difference between the actual and preset hydrogen ratios. As the pipeline height increases, the hydrogen concentration rises, resulting in a lower ratio at the bottom and a higher ratio at the top of the pipeline. The degree of stratification becomes more pronounced with increasing hydrogen blending ratio. The hydrogen concentration deviations between the base point and 1000 m were 0.5%, 0.9%, 1.2%, and 1.4% under hydrogen blending ratios of 10%, 20%, 30%, and 40%, respectively. However, given that building heights are typically below 100 m, the maximum deviation in the riser under a 40% hydrogen ratio is less than 0.15%, which can be considered negligible. Nevertheless, as experimental validation of such theoretical predictions under real building operating conditions remains limited, on-site measurements are still required to verify whether stratification occurs in practical high-rise gas distribution systems.

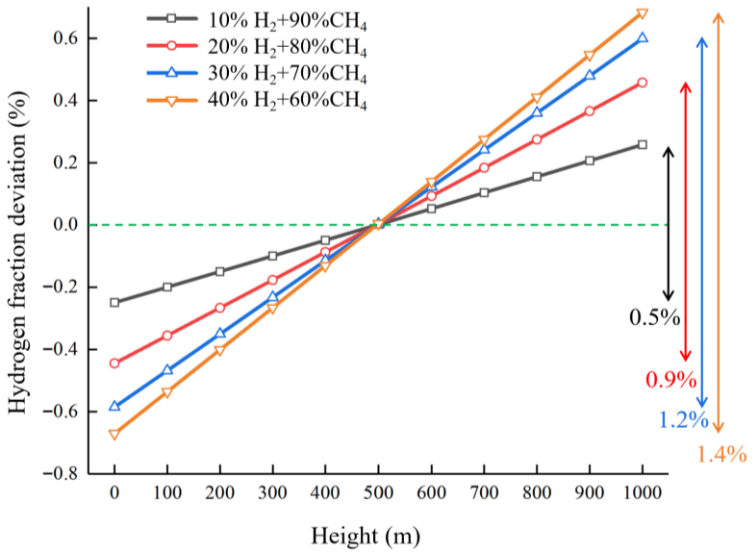


Figure 5. Effects of hydrogen ratio and pipeline height on gas stratification.

It should be noted that the above results correspond to a fully equilibrated gas mixture, whereas the diffusion process is generally slow and requires a long time to reach such equilibrium. The time required for equilibrium can be calculated according to the methods in [41,42]:

$$D = \frac{T^{1.765}}{P} \times 3.13 \times 10^{-10} \quad (7)$$

$$t \approx H^2/D \quad (8)$$

where D is the gas diffusion coefficient, m^2/s; P is the pressure inside the container, MPa; t is the time required for diffusion, s.

According to the calculation, the gas mixture in a 100 m high pipe at 20 °C and 3000 Pa would reach equilibrium after approximately 4.5 years. This theoretical timescale is provided to highlight the difficulty of achieving full stratification in practice, as residential gas risers rarely remain static for such extended periods. Under practical conditions, the standing period of the gas mixture is very short, so equilibrium cannot be achieved. As a result, the stratification observed in practice will be less significant than the calculated results. It can therefore be theoretically inferred that hydrogen injection into natural gas is unlikely to cause significant stratification within gas distribution systems.

The results of three on-site stratification experiments are presented in Figure 6. In this figure, different experiments are distinguished by color, with Experiment #1 (10% hydrogen ratio) shown in blue color, and Experiments #2 and #3 (20% hydrogen ratio) shown in yellow and green colors, respectively. At the beginning of the experiment, the pipe was filled with hydrogen-enriched natural gas through the hydrogen injection system, but the natural gas in the pipe was not fully purged, resulting in a slight difference between the initial gas compositions at the 3rd and 16th floors. In Experiment #1, after 16 h of standing, the methane–hydrogen ratio decreased at both the 3rd and 16th floors. In Experiment #2, after 16 h, the methane–hydrogen ratio increased at the 3rd floor but decreased at the 16th floor. In Experiment #3, after standing for 72 and 120 h, the methane–hydrogen ratio at the 3rd floor first increased and then decreased, while that at the 16th floor continued to increase. Only Experiment #2 exhibited a variation trend consistent with the theoretical prediction. The discrepancies observed in the other two experiments were likely due to measurement errors in Experiment #1 and the residual natural gas in the riser and branches, which increased the methane ratio at the 16th floor in Experiment #3. It should be noted that the absolute hydrogen concentration variations observed in all experiments were

very small (generally below 1%), which is close to the uncertainty range of on-site gas composition measurements. Under such conditions, residual gas and minor local mixing effects may influence the observed trends. However, the consistently small deviations confirm that no significant stratification occurs in high-rise building risers under practical operating conditions.

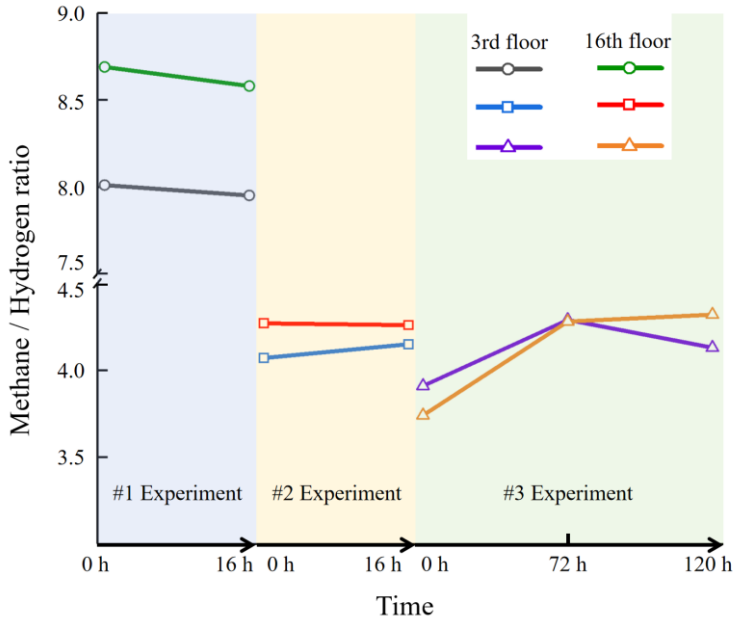


Figure 6. Variation in gas composition in the riser over time.

In Experiment #1, the variations in the methane–hydrogen ratio at the 3rd and 16th floors were minimal, with hydrogen ratio deviations of only 0.07% and 0.12%, respectively. The variations in Experiment #2 were also small, at 0.31% and 0.04%. In Experiment #3, the hydrogen ratio deviations were 0.64%, 0.03%, and 0.72%, respectively. Although minor composition differences were observed in the riser after standing for a period of time, the deviations were extremely small. It can therefore be concluded that gas stratification effects in high-rise building distribution systems can be neglected.

3.2. Additional Pressure in the Gas Distribution System

Considering the buoyancy caused by the density difference between the gas mixture and air, the theoretical additional pressure is proportional to the gas density and gravitational acceleration:

$$\Delta P_l = (\rho_{air} - \rho_{gas}) \times g \quad (9)$$

where ΔP_l is the theoretical additional pressure per unit height, Pa/m; ρ_{air} is the density of air, kg/m^3; ρ_{gas} is the density of the gas, kg/m^3.

The calculated theoretical additional pressures were 4.58 and 5.82 Pa/m under hydrogen ratios of 0% and 20%, respectively. Taking the 4th floor as the baseline, the variation in additional pressure with height and the measured values at the 16th floor are shown in Figure 7. In this figure, the parameter k represents the theoretical slope of the additional pressure-height relationship, i.e., the additional pressure increase per unit height of the riser. As height increases, the additional pressure also increases, exceeding 100 Pa. Therefore, its influence on the gas distribution system cannot be neglected. In the gas distribution system of Building #1, the riser diameter was reduced at the 8th floor to increase frictional pressure loss at higher floors and compensate for the additional pressure. Under the natural gas condition, the theoretical and measured values (4.58 Pa/m and 4.42 Pa/m) agree well, with only a 3.5% deviation. Under the 20% hydrogen ratio condition, the theoretical and

measured values (5.82 Pa/m and 5.31 Pa/m) show an 8.8% deviation, likely due to residual natural gas in the system, which reduced the actual hydrogen concentration below the nominal 20%. It can therefore be concluded that hydrogen blending increases the additional pressure in risers, and the theoretical predictions show good agreement with the experimental results. The observed deviations are within an acceptable range, and the measured additional pressures are consistently lower than the theoretical values, indicating that the theoretical calculation provides a conservative estimate suitable for engineering assessment.

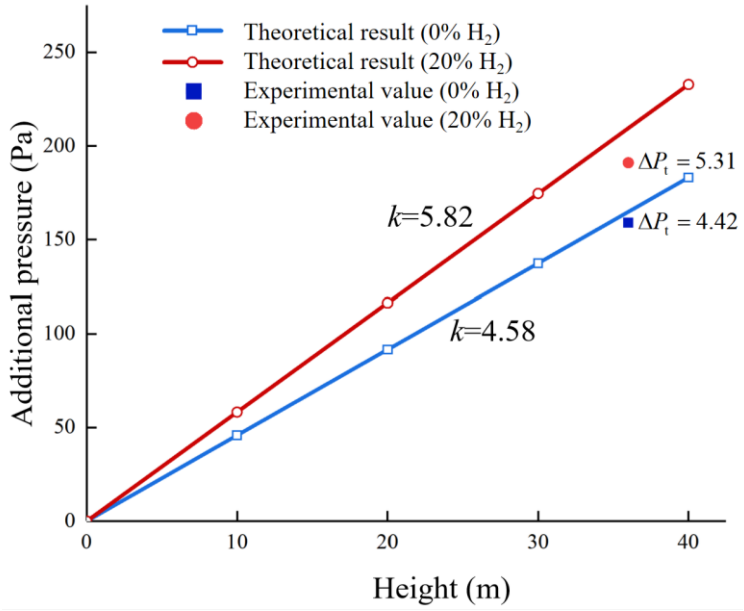


Figure 7. Comparison between measured and theoretical values of additional pressure.

The additional pressure induced by natural gas has already been considered in the system design so only the extra additional pressure caused by hydrogen blending needs to be evaluated in this study. According to theoretical calculations, every 10% hydrogen addition results in an extra additional pressure of 0.56 Pa/m. For a 100 m high building, a 20% hydrogen addition would increase the pressure at the highest point by about 112 Pa. Compared with the appliance operating pressure of 2000 Pa, the additional pressure of 518 Pa under natural gas conditions, and the allowable operating pressure fluctuation of 1500 Pa, this extra additional pressure is relatively small. Therefore, hydrogen blending does increase the additional pressure in high-rise building gas distribution systems, but the impact is relatively minor. If precise control of appliance inlet pressure is required, the outlet pressure of the building pressure regulator can be appropriately adjusted to compensate for this additional pressure. In practice, such adjustments should be implemented in accordance with the applicable operational procedures and technical regulations of the local gas utility.

3.3. Airtightness of Indoor Pipelines and Appliances

During normal operation, minor leakage may occur in gas pipelines and appliances due to gas diffusion through porous materials or microcracks. The diffusion coefficient of hydrogen is much higher than that of natural gas, so hydrogen addition in natural gas increases the leakage rate and may elevate safety risks. Leakage mechanisms are generally classified as pressure-driven and diffusion-driven [40]. For laminar pressure-driven leakage,

assuming incompressible flow with constant viscosity, the volumetric leakage rate can be expressed by the Hagen–Poiseuille equation:

$$Q = \frac{\Delta P \pi d^4}{128 \mu L} \tag{10}$$

where ΔP is the pressure drop across the leak, Pa; d is the diameter of the leak, m; μ is dynamic viscosity, Pa·s; L is the leak passageway, m.

For turbulent pressure-driven leakage, assuming a constant friction factor, the volumetric leakage rate can be calculated by Darcy's equation:

$$Q = 0.354\pi \frac{d^{2.5}\sqrt{\Delta P}}{\sqrt{f L \rho_{gas}}} \tag{11}$$

where f is the friction factor.

For diffusion-driven leakage, which is dominated by concentration gradients, the volumetric leakage rate can be expressed according to Fick's law:

$$Q = -\frac{1}{4}\pi d^2 D \frac{\partial c}{\partial x} V_m \tag{12}$$

where $\frac{\partial c}{\partial x}$ is the concentration gradient, mol/m; V_{m} is molar volume of gas, $\mathrm{m}^3/\mathrm{mol}$.

It can be seen that both pressure-driven and diffusion-driven leakages are strongly influenced by gas properties such as dynamic viscosity, density, and diffusion coefficient, indicating that hydrogen blending affects the leakage rate. The leakage rates of hydrogen-enriched natural gas under different hydrogen ratios were calculated using the three models described above. The ratio of the leakage rate of hydrogen-enriched methane to that of pure methane was plotted on the y-axis, as shown in Figure 8. As the hydrogen ratio increases, the gas leakage rate also increases. Among the three models, the leakage rate predicted by the diffusion model was the highest, followed by the turbulent model and the laminar model. At a 20% hydrogen ratio, the calculated increases were 43.0%, 10.1%, and 0.7%, respectively. In practical operation, the leakage process of pipeline is a combination of laminar and diffusion mechanisms. Therefore, hydrogen blending in natural gas is expected to increase the overall leakage rate.

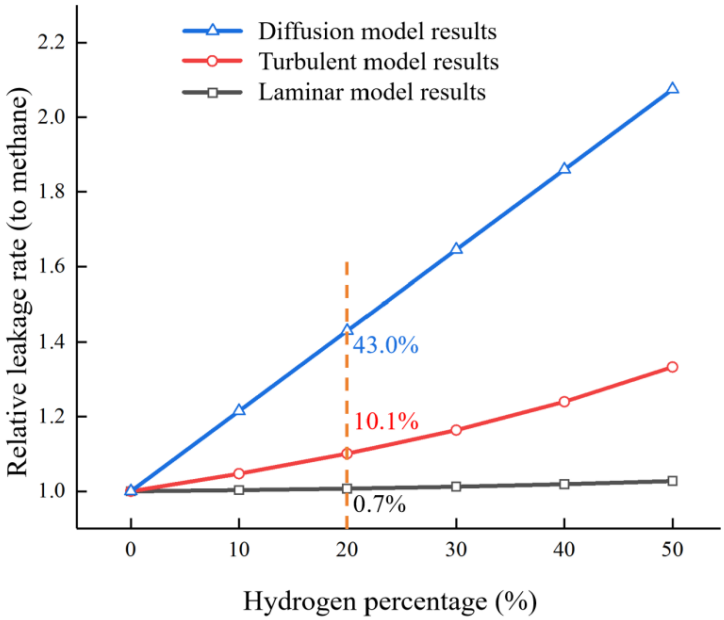


Figure 8. Effect of hydrogen addition on theoretical gas leakage rate.

The total leakage rates of the indoor gas system, including the pipeline downstream of the gas meter, gas appliances, and fittings, were obtained experimentally. The data were categorized by appliance service life into three groups: 1–5 years, 5–10 years, and 11–15 years, as shown in Figure 9. The service life of gas appliances was determined according to the manufacturing year or installation date indicated on the appliance nameplate or property management records. For systems with appliances under five years of service, the leakage rates under hydrogen ratios of 0%, 10%, and 20% were very similar, indicating that hydrogen addition had no significant effect. However, for systems with appliances over five years of service, the leakage rate increased noticeably with higher hydrogen ratios. At a 20% hydrogen ratio, the system pressure drop exceeded 100 Pa, and the average leakage rate was more than six times that under natural gas conditions. These results indicate that in systems with short service life, the pipelines, fittings, and sealing materials remain in good condition, effectively preventing gas leakage. In contrast, in long-service systems, material aging degrades airtightness, making the system less resistant to leakage of highly diffusive gases such as hydrogen.

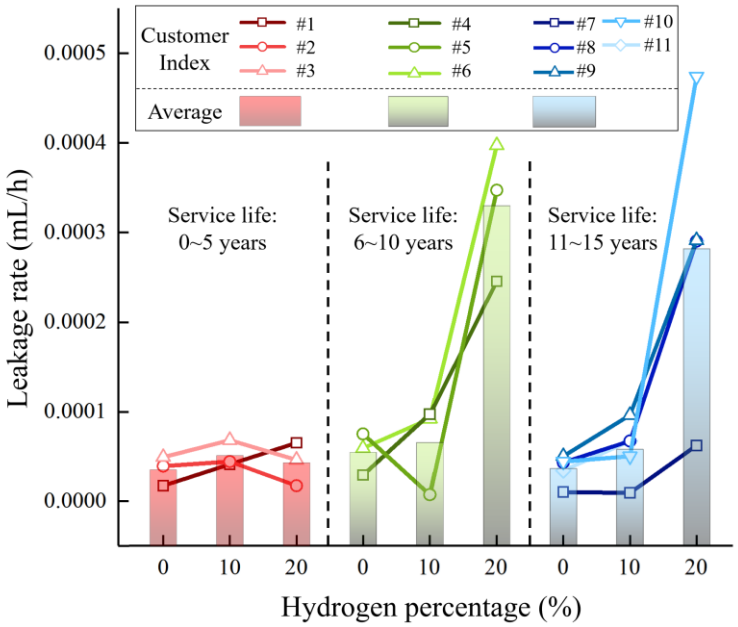


Figure 9. Effect of hydrogen addition on leakage rate of indoor gas system.

The strong correlation between leakage rate and cooktop service life indicates that leakage primarily occurs at the connection between the indoor gas pipeline and the cooktop. This connection involves dissimilar materials, a rubber hose and the metal gas inlet of the cooktop, which may loosen over time due to mechanical movement and material aging. Therefore, gas systems with long service-life appliances require greater attention in hydrogen blending projects, particularly regarding the pipeline–appliance connection, which should be subject to airtightness inspection under hydrogen-enriched natural gas. In addition, replacing aging hoses and re-securing the pipe–appliance connection can effectively improve the airtightness of the indoor gas system and reduce potential safety risks.

The results of the airtightness tests for in-service domestic gas meters are shown in Table 4. Under the 10% hydrogen ratio, all measured leakage rates were below 3 mL/h, meeting the required safety standards. Although abnormal values were observed for Residents #1 and #7, the overall data show an increasing trend in leakage rate with increasing floor height. This suggests that the higher gas pressure at upper floors may contribute to greater leakage. However, the leakage rate cannot be attributed to height alone, as

variations may also be influenced by individual meter conditions, installation differences, and sealing performance.

Table 4. Gas meter leakage rate under 10% hydrogen ratio.

No.	Floor	Hydrogen Concentration (ppm)	Methane Concentration (ppm)	Leakage Rate (mL/h)
1	1	0.019	15.4	1.01
2	2	0.03	3.6	0.09
3	2	0.011	4	0.12
4	2	0.015	5.3	0.22
5	5	0.045	9.6	0.55
6	6	0.046	11.8	0.73
7	8	0.044	3.2	0.05
8	11	0.036	40	2.93

3.4. Effectiveness of Domestic Gas Alarms

The effectiveness of domestic gas alarms may be influenced by hydrogen blending. Because hydrogen and natural gas have different flammability limits, the flammability range of the mixture changes after hydrogen addition, and the methane concentration corresponding to the flammability limit is changed as well. This can affect the accuracy of methane-based alarm detection. In addition, due to the lower density and higher diffusion coefficient of hydrogen, leaked hydrogen-enriched natural gas disperses more rapidly, which may result in delayed alarm response. Furthermore, many domestic gas alarms operate based on catalytic combustion sensing. The lower heating value of hydrogen weakens the catalytic reaction signal, thereby reducing detection sensitivity.

The flammability limits of hydrogen-enriched natural gas and the corresponding methane contribution are shown in Figure 10. The lower and upper flammability limits of methane are 5% and 15%, respectively. Under a 10% hydrogen ratio, the flammability range expands to 4.88–16.31%, and the methane concentration at the flammability limits becomes 4.39% and 14.68%. Under a 20% hydrogen ratio, the flammability range further expands to 4.76–17.78%, while the methane concentrations decrease to 3.81% and 14.22%. These results indicate that hydrogen addition widens the flammability range. However, since methane represents only part of the mixture, the methane concentration corresponding to the flammability limits is reduced. Domestic gas alarms are designed to detect the early stage of gas leakage that the gas concentration approaches the lower flammability limit. The methane concentration at the lower limit decreases by 0.61% and 1.19% under 10% and 20% hydrogen ratios, respectively. Although the alarm threshold of most domestic methane gas detectors is approximately 0.5%, there may still be safety risks if the methane concentration exceeds 1%, particularly for alarms with long service life or reduced sensitivity.

To evaluate alarm effectiveness under representative residential conditions, a controlled leakage source with a diameter of 1 mm was positioned 1 m below the gas alarm, consistent with typical household alarm installation practices. This configuration was selected to simulate a common indoor leakage scenario in residential kitchens, where gas leakage may originate from appliances or connecting fittings below the alarm location. The leakage position and installation height were intentionally fixed to reflect existing in-service residential conditions rather than to investigate all possible leakage configurations. The fixed leakage aperture and installation height allow a consistent and repeatable assessment of alarm response performance under different hydrogen blending ratios.

The test results indicate that the domestic gas alarms remained effective under hydrogen ratios of 0%, 10%, and 20%. The average response times were 20.1 s, 19.3 s, and 19.0 s, respectively, demonstrating that the alarms operated appropriately within the 0–20%

hydrogen range. If further improvement in the timeliness and accuracy of domestic gas alarms is required, hydrogen-compatible alarm systems and optimized installation layouts may be adopted. For example, adding additional detectors near the ceiling or implementing multi-point monitoring can enhance sensitivity to hydrogen due to its lower density and faster diffusion.

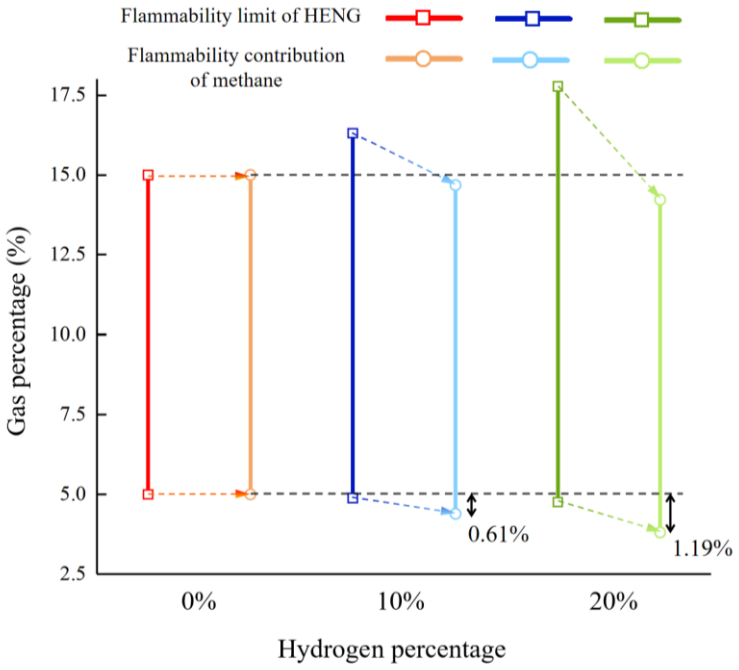


Figure 10. Effect of hydrogen addition on flammability limits and methane contribution.

4. Conclusions

This study conducted on-site demonstrations and experimental tests in two high-rise buildings in Weifang to investigate the impacts of hydrogen addition on natural gas distribution systems in residential high-rise buildings. The main conclusions are as follows:

(1) Theoretical analysis shows that for building heights below 1000 m, the maximum hydrogen concentration deviation in the riser under 20% hydrogen ratio is less than 0.9%, and full equilibrium would require approximately 4.5 years. Experimental results also show hydrogen concentration deviations below 1%. Therefore, gas stratification in high-rise building distribution systems can be considered negligible.

(2) Hydrogen blending increases the additional pressure in risers. Every 10% hydrogen blending results in approximately 0.56 Pa/m of extra additional pressure. Compared with appliance operating pressures and the normal allowable operating pressure fluctuation range, this extra additional pressure is relatively small.

(3) Systems with appliances under five years of service maintain stable airtightness under hydrogen blending, whereas systems with longer service life exhibit increased leakage due to material aging and loosening at pipeline–appliance connections. Therefore, gas systems with long service-life appliances require focused inspection and maintenance in hydrogen blending projects. Gas meter leakage rates under 10% hydrogen blending are below 3 mL/h, satisfying safety requirements.

(4) Domestic gas alarms remained responsive and reliable under 0–20% hydrogen ratios. Although hydrogen alters the flammability range, alarm detection accuracy and response time remained within acceptable limits for residential safety.

Author Contributions: Methodology, Y.X.; Validation, B.W. and Y.Z.; Investigation, H.X. and F.P.; Data curation, G.Z.; Writing—original draft, Y.X.; Writing—review and editing, X.H.; Visualization, B.W., Y.Z. and F.P.; Supervision, X.H.; Project administration, H.X., G.Z. and F.P. All authors have read and agreed to the published version of the manuscript.

Funding: This research was funded by the National Key R&D Program of China (No. 2022YFB4004400).

Data Availability Statement: The original contributions presented in this study are included in the article. Further inquiries can be directed to the corresponding author.

Conflicts of Interest: Author Guohong Zhang was employed by the company Weifang Gaoxin China Resources Gas Co., Ltd. The remaining authors declare that the research was conducted in the absence of any commercial or financial relationships that could be construed as a potential conflict of interest.

Nomenclature

d	diameter of the leak (m)
D	gas diffusion coefficient (m^2/s)
f	friction factor
F_i^{tot}	volume fraction of gas i in the whole system
$F_i(h)$	distribution of volume fraction of gas i at height h
g	gravitational acceleration (m/s^2)
h	height of gas (m)
h_f	floor height (m)
H	maximum height of the pipe (m)
L	leak passageway (m)
m_i	mass of the gas molecular (kg/mol)
M	molecular weight of the gas (g/mol)
Δm	total gas leakage mass (kg)
n	number of floors
P	gas pressure (Pa)
P_t	pressure at the bottom of the riser (Pa)
P_b	pressure at the top of the riser (Pa)
P_0	standard pressure (Pa)
$P_i(h)$	partial pressure of gas i at height h (Pa)
P^{tot}	average pressure of the whole system (Pa)
ΔP	pressure drop across the leak (Pa)
ΔP_t	additional pressure per unit height (Pa/m)
ΔP_l	theoretical additional pressure per unit height (Pa/m)
Q	volumetric leakage rate at standard conditions (m^3/s)
R	ideal gas constant
t	time required for diffusion (s)
T	gas temperature (K)
T_0	standard temperature (K)
V	pipeline volume (m^3)
V_m	molar volume of gas (m^3/mol)
τ	time interval between the initial and final measurements (s)
$\rho_i(h)$	normalized probability density of gas i at height h
ρ_{air}	density of air (kg/m^3)
ρ_{gas}	density of the gas (kg/m^3)
μ	dynamic viscosity (Pa·s)
$\frac{\partial c}{\partial x}$	concentration gradient (mol/m)

References

1. PBL Netherlands Environmental Assessment Agency. Trends in Global CO_2 and Total Greenhouse Gas Emissions. Available online: https://www.pbl.nl/en/publications/trends-in-global-co2-and-total-greenhouse-gas-emissions-2020-report (accessed on 21 December 2020).
2. Grams, C.M.; Beerli, R.; Pfenninger, S.; Staffell, I.; Wernli, H. Balancing Europe's wind-power output through spatial deployment informed by weather regimes. *Nat. Clim. Change* **2017**, *7*, 557–562. [CrossRef]
3. Midilli, A.; Dincer, I. Hydrogen as a renewable and sustainable solution in reducing global fossil fuel consumption. *Int. J. Hydrogen Energy* **2008**, *33*, 4209–4222. [CrossRef]
4. Hydrogen Council. Hydrogen Scaling Up: A Sustainable Pathway for the Global Energy Transition. 2017. Available online: https://hydrogencouncil.com (accessed on 4 December 2025).
5. Heid, B.; Linder, M.; Orthofer, A.; Wilthaner, M. Hydrogen: The Next Wave for Electric Vehicles. 2017. Available online: https://www.mckinsey.com/industries/automotive-and-assembly/our-insights/hydrogen-the-next-wave-for-electric-vehicles (accessed on 4 December 2025).
6. Ruijven, B.V.; Vuuren, D.P.V.; Vries, B.D. The potential role of hydrogen in energy systems with and without climate policy. *Int. J. Hydrogen Energy* **2007**, *32*, 1655–1672. [CrossRef]
7. Faye, O.; Szpunar, J.; Eduok, U. A critical review on the current technologies for the generation, storage, and transportation of hydrogen. *Int. J. Hydrogen Energy* **2022**, *47*, 13771–13802.
8. Staffell, I. Zero carbon infinite COP heat from fuel cell CHP. *Appl. Energy* **2015**, *147*, 373–385. [CrossRef]
9. Energy Research Partnership. Potential Role of Hydrogen in the UK Energy System. Available online: https://erpuk.org/wp-content/uploads/2017/01/ERP-hydrogen-report-oct-2016.pdf (accessed on 4 December 2025).
10. Yang, C.; Ogden, J.M. Determining the lowest-cost hydrogen delivery mode. *Int. J. Hydrogen Energy* **2007**, *32*, 268–286. [CrossRef]
11. Hart, D.J.; Howes, J.A.; Lehner, F.; Dodds, P.; Hughes, N.; Fais, B.; Sabio, N.; Crowther, M. Scenarios for Deployment of Hydrogen in Contributing to Meeting Carbon Budgets and the 2050 Target. 2015. Available online: https://www.semanticscholar.org/paper/Scenarios-for-deployment-of-hydrogen-in-to-meeting-Hart-Howes/7a94719c52fa0ea9672b8ac8e5721f38da76ce71 (accessed on 4 December 2025).
12. Deymi-Dashtebayaz, M.; Ebrahimi-Moghandam, A.; Pishbin, S.I.; Pourramenzan, M. Investigating the effect of hydrogen injection on natural gas thermo-physical properties with various compositions. *Energy* **2019**, *167*, 235–245. [CrossRef]
13. Vandewalle, J.; Bruninx, K.; Dhaeseleer, W. Effects of large-scale power to gas conversion on the power, gas and carbon sectors and their interactions. *Energy Convers. Manag.* **2015**, *94*, 28–39. [CrossRef]
14. Qadrdan, M.; Abeysekera, M.; Chaudry, M.; Wu, J.; Jenkins, N. Role of power-to-gas in an integrated gas and electricity system in Great Britain. *Int. J. Hydrogen Energy* **2015**, *40*, 5763–5775. [CrossRef]
15. Kippers, M.; De Laat, J.; Hermkens, R.; Overdiep, J.; Van Der Molen, A.; Van Erp, W.; Van Der Meer, A. Pilot project on hydrogen injection in natural gas on Island of Ameland in The Netherlands. *Int. Gas. Union. Res. Conf.* **2011**, *2*, 1163–1177.
16. Cuadrado, D.; García, G.; Gata, P.; Bermejillo, F.J.; Velasco, I.; Silveira, E.; Esnal, A.; Álava, I.; Mesanza, M.; Gómez, M.R.; et al. Integrative assessment of hydrogen-natural gas mixtures in energy grids: An overview of the H2SAREA project experience. *Int. J. Hydrogen Energy* **2025**, *142*, 697–711. [CrossRef]
17. Santoli, L.; Basso, G.L.; Bruschi, D. A small scale H2NG production plant in Italy: Techno-economic feasibility analysis and costs associated with carbon avoidance. *Int. J. Hydrogen Energy* **2014**, *39*, 6497–6517. [CrossRef]
18. ATCO. Fort Saskatchewan Hydrogen Blending Project. 2020. Available online: https://www.atco.com/en-ca/projects/fort-saskatchewan-hydrogen-blending-project.html (accessed on 4 December 2025).
19. Jaremko, G. Canadian Utilities Beginning Hydrogen Energy Field Tests. 2021. Available online: https://www.naturalgasintel.com/canadian-utilities-beginning-hydrogen-energy-field-tests/ (accessed on 4 December 2025).
20. AGIG. Australia's First Renewable Gas Blend Supplied to Existing Customers. 2021. Available online: https://www.agig.com.au/hydrogen-park-south-australia (accessed on 4 December 2025).
21. AGIG. A Pathway to a Cleaner Energy Future. 2021. Available online: https://www.agig.com.au/hydrogen-park-gladstone (accessed on 4 December 2025).
22. AGIG. A Globally Significant Decarbonisation Project. 2021. Available online: https://www.agig.com.au/hydrogen-park-murray-valley (accessed on 4 December 2025).
23. Peng, S.Y.; He, Q.; Peng, D.; Ouyang, X. Equilibrium distribution and diffusion of mixed hydrogen-methane gas in gravity field. *Fuel* **2023**, *358*, 130193. [CrossRef]
24. Azatyan, V.V.; Petukhov, V.A.; Prokopenko, V.M.; Timerbulatov, T.R. Possible gravitational stratification of components in mixtures of reaction gases. *Russ. J. Phys. Chem. A* **2019**, *93*, 986–987. [CrossRef]
25. Pitts, W.; Yang, J.; Blais, M.; Jayce, A. Dispersion and burning behavior of hydrogen released in a full-scale residential garage in the presence and absence of conventional automobiles. *Int. J. Hydrogen Energy* **2012**, *37*, 17457–17469. [CrossRef]
26. Badino, G. The legend of carbon dioxide heaviness. *J. Cave Karst Stud.* **2009**, *71*, 100–107.

27. Liu, C.; Pei, Y.; Cui, Z.; Li, X.; Yang, H.; Xing, X.; Duan, P.; Li, L.; Li, Y. Study on the stratification of the blended gas in the pipeline with hydrogen into natural gas. *Int. J. Hydrogen Energy* **2023**, *48*, 5186–5196. [CrossRef]
28. Marangon, A.; Carcassi, M. Hydrogen–methane mixtures: Dispersion and stratification studies. *Int. J. Hydrogen Energy* **2014**, *39*, 6160–6168. [CrossRef]
29. Su, Y.; Li, J.; Yu, B.; Wang, X.; Pu, M.; Wang, W.; Zhang, B. Study of Hydrogen Stratification Phenomena in Hydrogen-Blended Natural Gas Pipelines. *Renew. Energy* **2025**, *253*, 123603. [CrossRef]
30. Cen, K.; Su, L.; Wen, Y.; Song, B.; Zeng, Z.; Li, L.; Li, Q. Stratification characteristics of hydrogen-blended natural gas for gas risers inside residential users. *Int. J. Green Energy* **2024**, *21*, 3201–3217. [CrossRef]
31. Islam, A.; Alam, T.; Sheibley, N.; Edmonson, K.; Burns, D.; Hernandez, M. Hydrogen blending in natural gas pipelines: A comprehensive review of material compatibility and safety considerations. *Int. J. Hydrogen Energy* **2024**, *93*, 1429–1461. [CrossRef]
32. Mejia, H.A.; Brouwer, J.; Kinnon, M.M. Hydrogen leaks at the same rate as natural gas in typical low-pressure gas infrastructure. *Int. J. Hydrogen Energy* **2020**, *45*, 8810–8826. [CrossRef]
33. Mejia, H. Experimental Investigation of Hydrogen and Hydrogen/Methane Mixture Leakage from Low-Pressure Natural Gas Infrastructure. 2019. Available online: https://www.proquest.com/openview/163d00dfc4dc32ef5ac1b42f51ddd193/1?pq-origsite=gscholar&cbl=18750&diss=y (accessed on 4 December 2025).
34. Haeseldonckx, D.; D'haeseleer, W. The use of the natural-gas pipeline infrastructure for hydrogen transport in a changing market structure. *Int. J. Hydrogen Energy* **2007**, *32*, 1381–1386. [CrossRef]
35. Wilkening, H.; Barald, D. CFD modelling of accidental hydrogen release from pipelines. *Int. J. Hydrogen Energy* **2007**, *32*, 2206–2215. [CrossRef]
36. Xie, Y.; Qin, C.; Chen, Z.; Duan, P.; Guo, S. The impact of hydrogen addition to natural gas on flame stability. *Int. J. Hydrogen Energy* **2022**, *47*, 35851–35863. [CrossRef]
37. Rao, A. *Sustainable Energy Conversion for Electricity and Coproducts: Principles, Technologies, and Equipment*; Jon Wiley & Sons: Hoboken, NJ, USA, 2015. Available online: https://onlinelibrary.wiley.com/doi/book/10.1002/9781119064190 (accessed on 4 December 2025).
38. Glassman, I.; Yetter, R.A.; Glumac, N.G. *Combustion*; Academic press: Cambridge, MA, USA, 2014. Available online: https://www.sciencedirect.com/book/9780122858505/combustion (accessed on 4 December 2025).
39. *BS EN 437:2021*; Test Gases-Test Pressures-Appliance Categories. BSI Standards Publication: London, UK, 2021. Available online: https://webstore.ansi.org/Standards/BSI/BSEN4372021 (accessed on 4 December 2025).
40. Swain, M.; Swain, M.N. A comparison of H_2, CH_4 and C_3H_8 fuel leakage in residential settings. *Int. J. Hydrogen Energy* **1992**, *17*, 807–815. [CrossRef]
41. Shashkov, A.G.; Zolotukhina, A.F.; Fokin, L.P.; Kalashnikov, A.N. Transfer properties of mixtures of rarefied neutral gases. Hydrogen–argon system. *J. Eng. Phys. Thermophys.* **2010**, *83*, 188–208. [CrossRef]
42. Marrero, T.; Mason, E.A. Gaseous diffusion coefficients. *J. Phys. Chem. Ref. Data* **1972**, *1*, 3–118. [CrossRef]

Disclaimer/Publisher's Note: The statements, opinions and data contained in all publications are solely those of the individual author(s) and contributor(s) and not of MDPI and/or the editor(s). MDPI and/or the editor(s) disclaim responsibility for any injury to people or property resulting from any ideas, methods, instructions or products referred to in the content.